Polymer 51 (2010) 4110–4120

Contents lists available at ScienceDirect

Polymer

journal homepage: www.elsevier.com/locate/polymer

Solution properties of selectively modified hyperbranched polyesters

Susanne Boye, Hartmut Komber, Peter Friedel, Albena Lederer*

Leibniz-Institut für Polymerforschung Dresden e.V., Hohe Str. 6, 01069 Dresden, Germany

ARTICLE INFO

Article history:
Received 24 March 2010
Received in revised form
9 June 2010
Accepted 19 June 2010
Available online 7 July 2010

Keywords:
Hyperbranched
Fractionation
Polyesters

ABSTRACT

Simultaneous characterization of the degree of branching and molar mass on a molecular level for hyperbranched polymers is still strongly limited. Therefore model hyperbranched polyesters for development of new chromatographic techniques on the basis of 2,2-bis(hydroxymethyl)propionic acid were synthesized. The two types of OH-functionalities (linear and terminal) of the hyperbranched polymer were selectively modified using different protection groups. The modification of the terminal end groups was carried out using their diol character with the formation of a ketal ring without changing the chemical structure of the linear OH groups. In order to obtain completely non-polar polymer, the linear OH-units were functionalized with an acetyl group. The last modification step was the deprotection of the terminal end groups by removing the ketal ring. Fractions with various molar masses for each modification stage were obtained by preparative fractionation. Extensive characterization by SEC-MALLS, NMR spectroscopy, and viscosity measurements elucidated the dependence of the molecular shape in solution on the polarity. These results were supported by molecular dynamic simulations.

1. Introduction

Hyperbranched (hb) polyesters possess special properties and application aspects representative for the whole class of dendritic polymers [1,2]. An important advantage of hb systems is their cost-efficient and simple synthesis. Hyperbranched polyesters can usually be synthesized in a large scale by one-step melt polycondensation of commercially available AB_2 monomers. These polymers exhibit different properties compared to their linear analogues such as higher solubility in organic solvents and advantageous rheology characteristics, like low melt viscosity.

The profound characterization of the branching character of hb polymers is still a challenge due to their broad and multidimensional distributions, i.e. in molar mass and degree of branching (DB) simultaneously [3]. Information about the distributions in polymer samples is only accessible after their appropriate separation. One possibility is the Size Exclusion Chromatography (SEC), which separates polymers according to their hydrodynamic volume. Coupling SEC to a light scattering-detector provides reliable information about the molar mass distribution in the hyperbranched sample. However, co-elution of molecules with similar hydrodynamic volume but different DB could not be excluded.

The calculation of the DB being the most important, characteristic parameter for hb polymers is based on the ratio of the sum of dendritic (D) and terminal (T) units towards to the sum of all structure units (Scheme 1) including linear units (L) as proposed by Fréchet [4] (Eq. (1)).

$$DB_{Fréchet} = \frac{D + T}{D + T + L} \quad (1)$$

However, for low molar masses the amount of terminal units would be overestimated thus leading to a incorrect DB. Therefore, Frey [5] proposed the following equation:

$$DB_{Frey} = \frac{2D}{2D + L} \quad (2)$$

The common way to determine the DB according to these equations is the calculation based on the intensities of the NMR signals representing the different structure units. This pathway, however, provides only average values of DB.

Recently, progress has been made in developing separation methods according to the DB of star polymers or polymers with very long branches. The approaches were based on completely different principles – on the one hand interaction of end groups with the column material [6,7] and on the other hand topology-based separation in very narrow channels [8]. Because of the usually short branching distances in the hyperbranched architectures, the topology-based separation could not be applied to hb polymers. The two-dimensional liquid chromatography (2D-LC) proposed by Gerber et al. [6] can be successfully applied only to polymers with a defined number of end groups. Recently, we

* Corresponding author. Tel.: +49 351 4658 491; fax: +49 351 4658 565.
E-mail address: lederer@ipfdd.de (A. Lederer).

0032-3861/$ – see front matter © 2010 Elsevier Ltd. All rights reserved.
doi:10.1016/j.polymer.2010.06.037

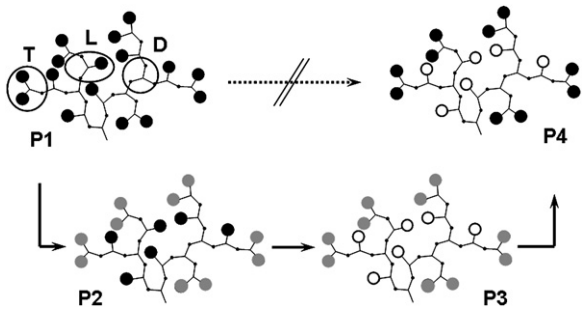

Scheme 1. Synthetic pathway for the selective modification of linear end groups of the hyperbranched polyester. Dark areas are representative for OH end groups, grey and white areas illustrate different protected end groups.

reported on our first studies on the separation of linear and gradually branched dendritic polyesters by interactive liquid chromatography based on their topology but not on the number of the end groups [7].

In the case of interactive liquid chromatography, similar interactions are expected for molecules with similar number and polarity of end groups but different degree of branching. It should be mentioned, that the degree of branching can exclusively be determined from the number of terminal groups, whereas the number of dendritic units is only one unit less than the number of terminal groups. Furthermore, the number of linear units approaches theoretically 50% of the whole amount of repeat units. Hence, a technique sensitive to the number and type of the end groups should provide information about the DB. In order to apply this separation technique according to DB, selective modification of the end groups of one type should be carried out switching them from polar to non-polar. The purpose of this selective modification is to deactivate the influence of the linear units and at the same time to tune the solution and interaction properties. Change in the solution properties leads to different elution behavior in liquid chromatography. Hence, by systematical change of the solvent content it might be possible to separate the hb polymers according to the branching degree.

In regard to this, tailored, selectively modified model polymers with a discrete molar mass and well characterized molecular properties in solution were the aim of this work. In order to determine solely the effect of the end groups, we followed the route of chemistry shown in Scheme 1. The aliphatic hb polyester based on 2,2-bis(hydroxymethyl)propionic acid (poly(BisMPA)) was used as model polymer for this work. As a representative example for AB_x ($x \geq 2$) polycondensation [9], poly(BisMPA) possesses broad and multidimensional distributions. The kinetics of formation of poly(BisMPA) was studied in detail by Malmström et al. [10,11]. Additionally, cyclization [12,13] and etherification [14] as side reactions were examined using analytical techniques, likes SEC, NMR spectroscopy or MALDI-TOF. Nevertheless, there is still no information available about how these parameters are related to each other and how they are distributed in one sample, despite the strong need for tuning the properties of these materials for different applications.

This polyester is commercially available by *Perstorp* under the trade name Boltorn® as a product with structure variations depending on the applied synthetic conditions like core moiety, slow monomer addition and end group modification. The application of this polymer type was extended into biomedicine [15] and photonics [16] and nanotechnology [17] with specially functionalized dendritic and hb polyesters as provided by *Polymer Factory*. Nevertheless, the strong academic interest into Boltorn®-type polymers continues, due to the strong need for understanding the structure–property relationships for improvement of material properties.

For the provided utilization as model polymer for 2D-LC method development selective modification of poly(BisMPA) was carried out. In case of statistically branched polymers this is not a trivial task because of equal reactivity of linear and terminal end groups especially in case of ideal statistics during the polycondensation [9]. Therefore, modification of the linear functionalities is not directly possible, but it is feasible using selective end group modification depending on sterical properties. Comprehensive work on this kind of modification of hb polyglycerols has been carried out by Haag et al. [18] showing the strong influence of the end group type on solubility and thermal properties.

In the case of poly(BisMPA) the two types of hydroxyl functionalities were modified with different protection groups. The formation of a ketal ring was carried out to switch the polarity of the terminal units by using 2,2-dimethoxypropane (DMP) without changing the chemical structure of the linear end groups. In order to obtain completely non-polar polymer, the linear OH-units were functionalized with acetyl groups. The last step of the selective modification was the deprotection of the terminal functionalities by using an acidic ion exchange resin to remove the ketal ring. Preparative fractionation was carried out for each modification stage to obtain fractions consisting of different, discrete molar masses which were subsequently characterized. The aim of our work was the detailed investigation of the molecular solution parameters and the tuning effect of the functional groups on the shape of the dissolved hb molecule.

2. Experimental section

2.1. Materials

2,2-Bis(hydroxymethyl)propionic acid (BisMPA) was purchased from Lancaster, UK. Dowex™ ion exchange resin 50 W-X2 and all other chemicals were obtained at the highest purity available from Sigma Aldrich and used without further purification, except tetrahydrofurane (THF), which was used freshly distilled.

2.2. Methods

^{1}H and ^{13}C NMR spectra were recorded on a Bruker DRX 500 spectrometer operating at 500.13 MHz for ^{1}H and 125.74 MHz for ^{13}C using DMSO-d_6 as solvent, lock, and internal standard [δ (^{1}H) = 2.50 ppm; δ (^{13}C) = 39.6 ppm]. Quantitative ^{13}C NMR spectra were obtained using inverse-gated decoupling, 90° pulses, and a pulse delay of 12 s. The content of different structural units and the DB values were determined for **P1** (Schemes 1 and 2) from corresponding signals of the quaternary carbon C_4 as described by Komber et al. [14]. The absolute error in determination the mole fractions of the different units is about 2 mol%.

The Size Exclusion Chromatography (SEC) system (pump: WGE Dr. Bures, Germany) was coupled to a viscosity/differential refractive index (RI) detector (ETA-2020, WGE Dr. Bures, Germany) and a multi angle laser light scattering-detector (MALLS) Dawn®EOS (Wyatt Technologies, USA). The measurements were carried out with a column PLgel, 5 μm MIXED-C, 300 × 7.5 mm (Varian, UK). Sample concentration in THF was approximately 2 mg/mL. THF as eluent for all measurements was used. The flow rate was 1.0 mL/min at a temperature of 25 °C. In order to achieve complete information about the molar mass distribution of the samples, fit of the molar mass/elution volume dependence in the whole elution region covered by the RI signal has been applied. The *dn*/*dc* was determined by estimating 100% mass recovery.

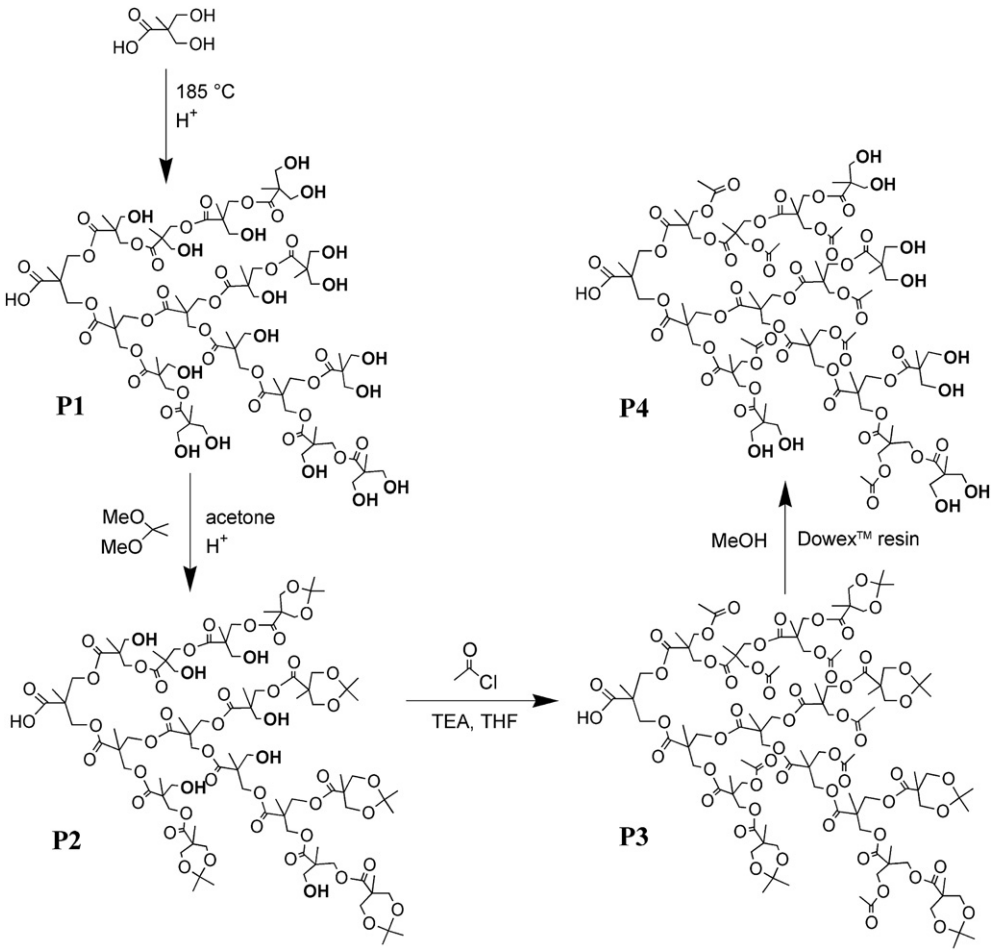

Scheme 2. Synthetic steps for selective modification of linear and terminal end groups.

The viscosity measurements were performed with a Berger-Deckert-Ubbelohde-viscometer at 25 °C with THF as solvent. The reduced viscosity at a concentration of 1.0 mg/ml was used instead of the intrinsic viscosity because of the small fraction amounts available. According to our previous experience with identical polymers [19] the values of the reduced viscosity at this low concentration are representative for the intrinsic viscosity of the polymer sample.

The fractions were obtained at ambient temperature by extracting the polymers with a gradient of solvent/non-solvent (elution fractionation). The applied non-solvent was *n*-hexane and the solvent was distilled THF. For optimization of the elution process, small scale fractionation of 50 mg polymer sample was performed.

Preparative fractionation: Glass beads (Ballotini, 0.1–0.2 mm diameter) were coated with the corresponding polymer (1.9–2.2 g) from THF solution. The fractionation column with 100 cm length and 2.7 cm diameter was filled with *n*-hexane and the coated glass beads. The eluent gradient of THF in n-hexane was started at 0% and was increased to 100% at a flow rate of approx. 2.5 mL/min. The fractions were collected in flasks and the solvent was removed under reduced pressure. The fractions were dried *in vacuo* at 40 °C for at least 24 h for subsequent investigations.

The molecular dynamic simulations were performed applying the software package GROMACS, version 3.3.3 [20]. The system type was chosen as an NpT ensemble with a constant pressure of 101.3 kPa and a constant temperature of 298 K as the thermodynamic standard state applying the Berendsen coupling method [21]. The used force field was G43B1, the cut-off radii for all the nonbonding interactions, i.e., the Van der Waals and the Coulomb interactions was set to 1.8 nm and the dielectric constant ε_r to 1.0. The atomic charges of the solvent THF and the monomer unit BisMPA were calculated by an ab initio quantum mechanical optimization method with the software package GAMESS [22] using the basis set 6–31 G. The monomer unit was applied to build the model for the hyperbranched polymer **P1**. Similar to the real synthetic procedure this model was modified to receive models for the **P2**, **P3** and **P4** by exchanging the proton pairs of the T standing hydroxyl group pairs by an acetal residuum and/or the protons of the L standing hydroxyl groups by acetate residues (Scheme 2). The corresponding four polymer models were dissolved in THF solvent in order to receive a diluted polymer solvent system. These four systems were energetically minimized by a steepest descent method and relaxed to the thermodynamic standard state afterwards including a following 300 ps simulation time period for the evaluation of the time average ensemble of the relaxed state.

2.3. Synthesis of ***P1*** by one-pot melt polycondensation

BisMPA (51 g, 0.38 mol) and *para*-toluene sulfonic acid (*p*-TSA; 92.5 mg, 0.13 mol%) were heated to the reaction temperature of 180–185 °C in a two-necked flask with a magnetic stirrer and gas inlet and outlet tubes. During the first 2 h a constant flow of argon was applied for removing the water formed during the reaction followed by vacuum (10^{-2} mbar) for 8 h. The product was cooled

down and dissolved in THF. For purification, the polymer was precipitated two times from cold diethyl ether and the white solid was dried at 40 °C *in vacuo*.

P1 ^{1}H NMR (DMSO-d_6, ppm): 1.02 (H_1 – T); 1.08 (H_1 – L); 1.17 (H_1 – D); 3.35–3.55 (H_4 – T, L); 4.00–4.20 (H_5 – L, D); 4.60 (OH, T); 4.90 (OH, L).

^{13}C NMR (DMSO-d_6, ppm): 16.5–17.5 (C_1 – T, L, D); 46.4 (C_2 – D), 48.4 (C_2 – L), 50.4 (C_2 – T); 63.5–64.4 (C_4 – T, L); 64.4–66.8 (C_5 – L, D), 171.4–172.3 (C_3 – D), 172.3–173.8 (C_3 – L), 173.8–175.0 (C_3 – T) (See Scheme 3).

2.4. Protection of terminal functional groups (*P2*)

The polymer **P1** (30 g, 4 mmol), acetone (150 mL), 2,2-dimethoxypropane (DMP; 0.13 mol, 1:1 M ratio according to diol (T) units) and *p*-TSA (26 mg) were reacted in a two-necked round-bottom flask under argon flow at room temperature for 24 h. After neutralization of the mixture with $NH_{3(aq.)}$/EtOH (50:50), the acetone was evaporated. For purification, the polymer was dissolved in CH_2Cl_2 and extracted with distilled water two times. The organic phase was dried with sodium sulfate and the solvent was removed under reduced pressure. The white solid of **P2** was dried at 40 °C *in vacuo*.

P2 ^{1}H NMR (DMSO-d_6, ppm): 1.00–1.12 (H_1 – L, T_p); 1.17 (H_1 – D); 1.25 and 1.34 (H_8 – T_p); 3.35–3.55 (H_4 – L), 3.58 and 3.99 (H_6 – T_p); 4.00–4.20 (H_5 – L, D), 4.90 (OH, L).

^{13}C NMR (DMSO-d_6, ppm): 16.5–17.5 (C_1 – L, D); 17.8–18.5 (C_1 – T_p); 21.3–22.5 and 24.8–26.0 (C_8 – T_p); 41.5 (C_2 – T_p), 46.4 (C_2 – D), 48.4 (C_2 – L), 63.5–64.4 (C_4 – L); 64.4–66.8 (C_5 – L, D), 65.2 (C_6 – T_p); 97.5 (C_7 – T_p); 171.4–172-3 (C_3 – D), 172.3–173.8 (C_3 – L, T_p). (See Scheme 3). Degree of protection: 97%.

2.5. Modification of linear functional groups (*P3*)

20 g of **P2** (1.4 mmol) were dissolved in distilled THF (35 mL). In a three-necked round-bottom flask with a magnetic stirrer, thermometer and dropping funnel, the solution was cooled down to 0–4 °C and triethylamine (TEA) (11 mL) and acetyl chloride (AcCl; 0.1 mol, 1:1 M ratio according to linear OH groups) were added to the reaction system drop by drop over 2 h. Afterwards the solution was stirred at room temperature for 22 h. The whole reaction was accomplished under argon atmosphere to avoid the hydrolysis of the acid chloride. After filtration of the triethylammonium chloride salt and removal of THF, a yellow oily polymer was obtained and dissolved in CH_2Cl_2 (40 mL). The solution was extracted with a sodium carbonate solution (10 vol%) for two times. The organic phase was dried with Na_2SO_4. Afterwards it was filtered off and the solvent was removed under reduced pressure. The yellow polymer **P3** was dried at 40 °C *in vacuo*.

P3 ^{1}H NMR (DMSO-d_6, ppm): 1.00–1.20 (H_1 – L_p, T_p, D); 1.25 and 1.34 (H_8 – T_p); 1.99 (H_{11} – L_p); 3.58 and 3.99 (H_6 – T_p); 4.00–4.30 (H_5 – L_p, D; H_9 – L_p).

^{13}C NMR (DMSO-d_6, ppm): 16.5–17.5 (C_1 – L_p, D); 17.8–18.5 (C_1 – T_p); 20.3 (C_{11} – L_p); 21.3–22.5 and 24.8–26.0 (C_8 – T_p); 41.5 (C_2 – T_p), 45.5–46.5 (C_2 – L_p, D; C_9 – L_p), 64.5–66.8 (C_5 – L_p, D), 65.2 (C_6 – T_p); 97.5 (C_7 – T_p); 169.8 (C_{10} – L_p); 171.0–173.5 (C_3 – L_p, T_p, D). (See Scheme 3). Degree of protection: > 98%.

2.6. Deprotection of terminal groups (*P4*)

The polymer **P3** (5 g, 0.2 mmol) was dissolved in methanol (250 mL). Under constant argon flow, stirring and cooling with water and ice, two spatula tips of Dowex™ resin were added to the solution and stirred for further 22 h. After filtration of the ion exchange resin the methanol was removed under reduced pressure. For purification, the yellow oily polymer was dissolved in CH_2Cl_2 and extracted with water three times. Subsequently, the solvent was removed and the yellow polymer **P4** was dried at room temperature *in vacuo*.

P4 ^{1}H NMR (DMSO-d_6, ppm): 1.02 (H_1 – T); 1.07 (H_1 – L_p); 1.17 (H_1 – D); 1.99 (H_{11} – L_p); 3.35–3.50 (H_4 – T); 4.00–4.30 (H_5 – L_p, D; H_9 – L_p); 4.60 (OH, T).

^{13}C NMR (DMSO-d_6, ppm): 16.5–17.5 (C_1 – T, L_p, D); 20.3 (C_{11} – L_p); 45.5–46.5 (C_2 – L_p, D; C_9 – L_p), 50.4 (C_2 – T); 63.8 (C_5 – T); 64.5–66.5 (C_5 – L_p, D), 169.8 (C_{10} – L_p); 171.0–173.5 (C_3 – L_p, D); 173.8–175.0 (C_3 – T). (See Scheme 3). Degree of deprotection: ~100%.

2.7. Synthesis of linear polyester

The synthesis of the linear polyester is explained in detail in the work of Schallausky [19]. The following general procedure was applied: Equimolar reaction of 3-ethyl-3-methylglutaric acid and 2,2-diethyl-1,3-propanediol with p-toluene sulfonic acid as catalyst in toluene was performed. Azeotropic distillation and subsequent solvent evaporation led to the product, which was afterwards dissolved in methylene chloride. Extraction from water and drying gives the pure oligomer. Higher molar masses were obtained after polycondensation in melt *in vacuo* with dibutyltin diacetate as catalyst. Different reaction temperatures (between 120 and 180 °C) and different reaction times led to a portfolio of linear polyesters with different molar masses.

3. Results and discussion

3.1. Synthesis and characterization

The synthesis of the aliphatic polyester with OH end groups (**P1**, Scheme 2) was carried out according to the well known self-condensation in reactive melt yielding products with molecular properties as described in the work of Magnusson et al. [11].

The polymer structure was analyzed by ^{1}H and ^{13}C NMR spectroscopy (Fig. 1) taking into account side reactions as described by Komber et al. [14]. Besides the signals of the regular structure (see

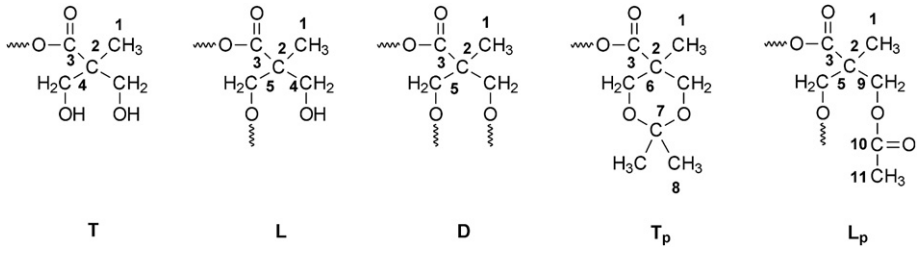

Scheme 3. Substructures of the studied polymers **P1** (T, L, D), **P2** (T_p, L, D), **P3** (T_p, L_p, D), and **P4** (T, L_p, D) with atom numbering for NMR signal assignment.

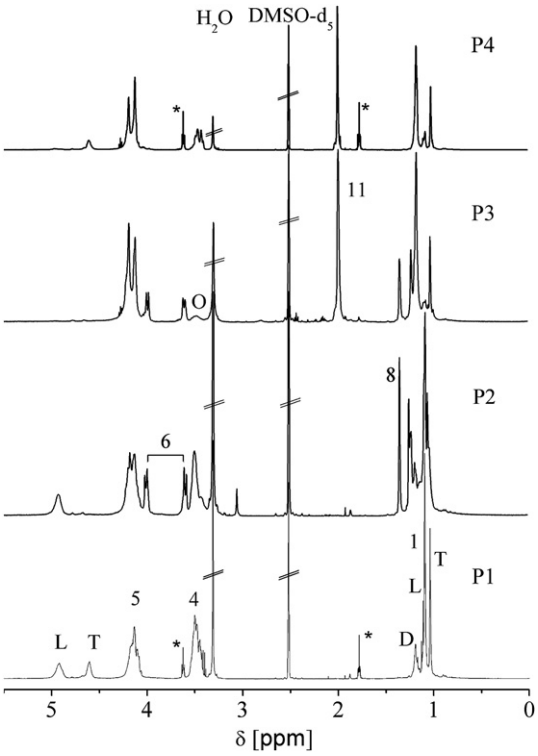

Fig. 1. ^{1}H NMR spectra of **P1**–**P4** in DMSO-d_6 (*: traces of THF; O: $-CH_2-O-CH_2-$). T: terminal units; L: linear units; D: dendritic units; numbering according to Scheme 3.

Experimental part and Scheme 3) also signals of low intensity, characteristic for linear and dendritic focal groups and ether structures, were observed. The occurrence of focal group signals correlates with relatively low M_n = 3700 g/mol as determined by SEC-MALLS (Table 1). Etherification of two hydroxyl groups is a side reaction described for poly(BisMPA) from acid-catalyzed polycondensations [13,14]. The content of ether groups which can be either intra- or inter-molecular was determined by quantitative ^{13}C NMR. The intensity ratio of the ether methylene group signal at 72.9 ppm to the sum of all methylene groups gives a content of about 4 mol% similar to previous results [14]. The relatively low amount of ether bonds was not expected to influence the solution properties of the polymer significantly. The degree of branching determined from the intensities of the quarternary carbon signals [14] according to eqs. (1) and (2) was found to be $DB_{Fréchet}$ = 0.45 and DB_{Frey} = 0.44. Although these values differ from the theoretically expected DB of 0.5 [9], they are typical for hyperbranched poly (BisMPA) and indicate non-ideal statistics during the reaction as previously discussed [11,14].

Table 1
Degree of modification, yield, molar masses, and refractive index increments of **P1**–**P4**.

Polymer	Modification degree [%]	Yield [%]	$M_{n,\,theor}$ [a] [g/mol]	M_n [b] [g/mol]	M_w [b] [g/mol]	dn/dc [c] [mL/g]
P1	–	97	–	3700	27 300	0.068
P2	97	93	3950	3100	34 700	0.070
P3	>98	93	4570	5400	36 200	0.052
P4	~100	51	4320	2500	10 600	0.055

[a] Theoretical calculation relative to **P1** (M_n = 3700 g/mol, degree of polymerization 30 and amount of end groups calculated from ^{13}C NMR: 22% terminal and 55% linear units).
[b] Molar mass determined by sample specific calibration.
[c] Refractive index increment (dn/dc) determined by SEC-MALLS.

As a next reaction step, the selective protection of the terminal groups of **P1** was performed by conversion with 2,2-dimethoxypropane leading to **P2** (Schemes 1 and 2). This reaction is widely used to protect 1,2- and 1,3-diols as cyclic *O,O*-isopropylidene acetals [23]. As the terminal units of poly(BisMPA) are 1,3-diols (Schemes 2 and 3), they react under formation of a six-membered ring. The linear units are not involved in this reaction. The progress of the reaction can be followed via ^{1}H NMR spectroscopy by appearance of signal pairs caused by axial and equatorial methyl (1.25 and 1.34 ppm) and methylene protons (3.58 and 3.99 ppm) and by disappearance of the phenolic protons signal of T units at 4.60 ppm (Fig. 1). The existence of linear acetals was not observed. The degree of conversion was determined from the intensity of the residual C_4 signal of T units compared to its intensity in **P1** and found to be 97%.

The remaining hydroxyl groups of linear units were protected by conversion with acetyl chloride using triethylamine for neutralization of the formed HCl in order to prevent cleavage of the acetal protection group of the T units under acidic conditions. As result of this esterification polymer **P3** was obtained without any hydroxymethyl groups as indicated by disappearance of the characteristic signals in the ^{1}H NMR (3.35–3.55 ppm) and ^{13}C NMR spectra (63.5–64.4 ppm). The remaining ^{1}H NMR signal at 3.45 ppm (Fig. 1) is caused by the ether methylene protons as confirmed by 2D NMR. The residual content of unprotected L groups was found to be lower than 2%.

Finally, the polymer **P4** with deprotected, terminal OH groups but protected linear OH groups was obtained from **P3** by selective removal of the cyclic *O,O*-isopropylidene acetals groups under acidic conditions. Complete disappearance of the typical signals for this unit proved recovery of the terminal OH groups without changes in the non-polar linear units (Fig. 1).

Whereas quite high yield of **P1**–**P3** was obtained (Table 1), the yield of **P4** in the last reaction step was only 51% due to hydrolysis. The weight average molar masses (M_w) of **P1**–**P3** listed in Table 1 show reasonable increase whereas strong drop in M_w was found for **P4**. This fact is a clear indication that during the last reaction step loss of high molar mass species has occurred. Partial hydrolysis of ester bonds under acidic conditions leads to cleavage of dendritic units resulting in new, unprotected linear OH groups. Obviously, the number of these new groups is relatively low, since no increase of the ^{1}H and ^{13}C NMR signal intensities was observed. Further hydrolysis of linear units could lead to OH-functionalized T units, which, however, would not influence negatively the polymer characteristics for the purpose of our study.

The theoretically calculated number average molar masses ($M_{n,\,theor}$) of **P2**–**P4** listed in Table 1 are calculated on the basis of the experimentally determined M_n for **P1**. The deviation of the experimental M_n from $M_{n,\,theor}$ is relatively low for **P2** and **P3**. The deviation for **P4** can be explained with the hydrolysis as side reaction, responsible also for its lower yield and molar mass as mentioned above. The molar mass distributions of **P1**–**P4** are shown in Fig. 2a resulting from the normalized refractive index (RI) chromatograms which are calculated via molar mass determination by light scattering (MALLS) detection (see Experimental section). The shape of the chromatograms is similar for **P1**–**P3**, whereas for **P4** the amount of higher molar mass species is strongly decreased as discussed above.

The differences in the chemical character of the polymers could be observed in addition following the values of the refractive index increment values (dn/dc in Table 1) in THF at room temperature. These values are different for every polymer according to the modification of the chemical structure. The protection of the terminal end groups leads to slight decrease of dn/dc in **P2** compared to **P1**. Their deprotection leads in turn to the slight

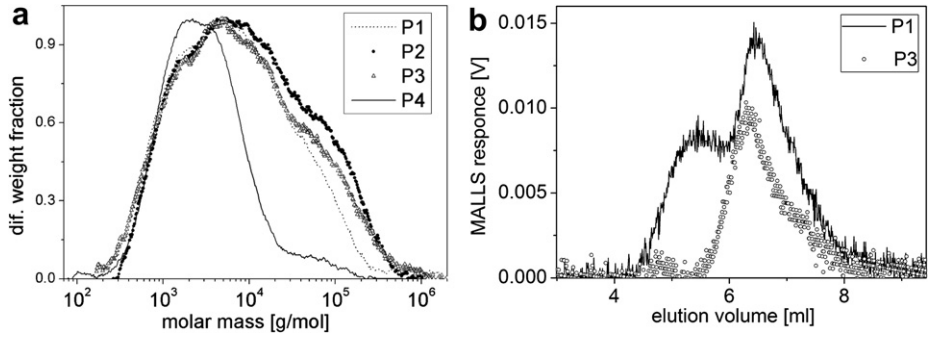

Fig. 2. a) Molar mass distribution according to RI signal of **P1**–**P4**; b) SEC-MALLS chromatograms of **P1** and **P3**. MALLS signal of **P3** has lower intensity despite the higher molar mass because of lower *dn*/*dc* (Table 1) and lower concentration of the injected sample.

increase of this value in **P4** compared to **P3**. Stronger influence on the *dn*/*dc* values have obviously the linear end groups, since after their modification, *dn*/*dc* drops stronger in **P3** compared to **P2**. This effect can be easily explained with the higher number of linear (55%) compared to the terminal repeat units (23%) and their stronger effect after modification, respectively.

MALLS information about the lower molar mass region cannot be obtained having broadly distributed molar masses. In order to enable interpretation of the complete distribution, special treatment and MALLS data using a fit of the molar mass/elution volume dependence for the whole RI-chromatogram was performed. Despite the relatively low intensity of the light scattering signal due to the low *dn*/*dc* values, clearly linear molar mass/elution volume dependence was obtained, showing complete elution of the sample according to molar mass. Additionally to the main MALLS-peak of **P1** in Fig. 2b, a strong shoulder at lower elution volumes is clearly visible corresponding to species in very low concentration, not detected by RI detector. The shoulder for **P1** is representative for **P2** and **P4** as well and corresponds to aggregates due to hydrogen bonding of the polar end groups, investigated in detail for Boltorn®-type polymers by Žagar et al. [24]. The disappearance of this shoulder in the MALLS-response of the completely non-polar **P3** supports this fact (Fig. 2b). Obviously the aggregation behavior of the polymers is not influencing their reactivity as can be concluded from the high modification degree obtained in all reaction steps.

3.2. Elution fractionation

For method development in chromatography, polymers with well-defined molecular properties are essential. Therefore, series of samples with narrowly distributed molar masses from every type of the modified polymers are required. Furthermore, detailed investigation of the properties of these polymers in solution should give us an insight into the influence of the polarity on interactions with solvent or solvent mixture. In order to collect all this information, elution fractionation of **P1**–**P4** was performed. The fractionation was carried out on a preparative scale as described in previous reports [25,26] obtaining fractions in sufficient amount (200–400 mg) for further analytical investigations. Compared to the broadly distributed starting materials we obtained molar mass distributions (M_w/M_n) below 2 (Table 2). The low polydispersities (PDI) as well as the variety of molar masses of the polymer fractions (**P1**–**P4**, Fig. 3) are an essential requirement for their suitability as model materials for separation method development.

In order to evaluate the elution behavior of the polymers comparable solvent gradients of THF/*n*-hexane were used. Clear separation according to molar mass for all polymer types was identified as shown in Fig. 3. Further information about the chemical identity and branching degree was obtained by NMR investigations of all samples. Chemically identical structures were found for the fractions of every polymer type. As an example, the molar masses and the degrees of branching of selected **P1** fractions are listed in Table 2. At lower fraction numbers the MALLS signal intensity was too low for determination of M_w due to low molecular size and *dn*/*dc*.

As expected, the molar mass M_w increases with increasing fraction number but the PDI remains quite small and comparable for all fractions. Due to the low amount of polymer of each fraction the DB could not be determined by ^{13}C NMR but was determined from CH_3 signal intensities of the ^1H NMR spectra. However, these values do not reflect the correct DB because the methyl signals of the linear and terminal unit overlap with signals from ether units resulting in an overestimation of L and T and thus in an underestimation of DB [14]. Therefore, the values were named as apparent degree of branching (DB_{app}). Because ether groups were confirmed for **P1** and should be present in the molar mass region represented by fractions 14–20 their DB_{app}s are smaller than the values obtained for non-fractionated **P1** by ^{13}C NMR but comparable with the DB_{app}s determined for **P1** by ^1H NMR. Furthermore, the DB values of all samples are within the experimental error of ±2% and no fractionation according to the degree of branching can be identified. Thus, the polymers were separated solely according to molar mass. However, this fact does not exclude the possibility that different degrees of branching are existent in one sample and that elution with different eluents would lead to separation according to branching, which is the target of our further studies.

Detailed comparison of the fractionation process of **P1**–**P4** demonstrates well distinguishable differences in their elution behavior. Fig. 4 shows the dependency of obtained fraction yield on the solvent gradient during the elution fractionation.

Table 2
Molar mass distributions and apparent degrees of branching (DB_{app}) of selected **P1** fractions.

Fraction no.	M_w[a] [g/mol]	PDI[a] (M_w/M_n)	$DB_{app,\ Fréchet}$[b]	$DB_{app,\ Frey}$[b]
14	6000	1.43	0.42	0.34
15	7400	1.48	0.42	0.34
16	9500	1.64	0.41	0.34
18	15 500	1.91	0.43	0.34
19	21 100	1.69	0.44	0.35
20	25 200	1.74	0.42	0.34
P1 Starting material	27 300	7.38	0.43	0.39

[a] Determined by sample specific calibration (see Experimental section).
[b] Calculated from ^1H NMR spectra.

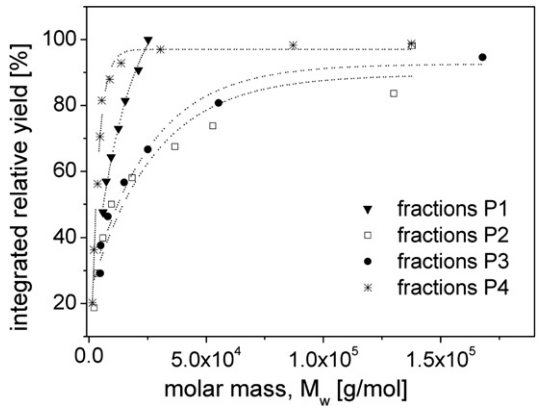

Fig. 3. Molar mass development in the fractions of **P1**–**P4** depending on the eluted polymer amount.

The influence of the end group polarity on the elution process can easily be identified: the OH end groups resist elution with THF/n-hexane gradient stronger than the completely non-polar end groups of **P3**. As a result, at 100% THF content **P1** is still not completely eluted, whereas **P3** achieves complete elution already at 64% THF. Furthermore, distinguishing behavior for **P2** and **P4** can be observed, in which polar and non-polar end groups are combined in one molecule. This fact refers to a characteristic influence of the modified polymer units, depending on their type – terminal (**P2**) or linear (**P4**). Hence, it can be concluded that selective switching of the end group polarity of hyperbranched aliphatic polyester leads to well-tunable elution properties of the macromolecule. This is supported by the values listed in Table 3, which correspond to a fixed THF content of the eluent at 60%. Fully modified end functionalities (**P3**) lead to much faster elution reaching 100 times higher molar masses than the OH-terminated polymer at the same elution conditions. Obviously, separation of discrete molecular size at the same conditions is taking place. However, the separation depends on the strength of the eluent–polymer interactions correlating with the eluted polymer yield. These results are first indication that the prepared substances are suitable as model polymers for separation by interaction liquid chromatography.

3.3. Dilute solution properties

Deeper understanding of the changes in the molecular parameters depending on the end group modification could be achieved by investigation of the compactness of the molecules in solution.

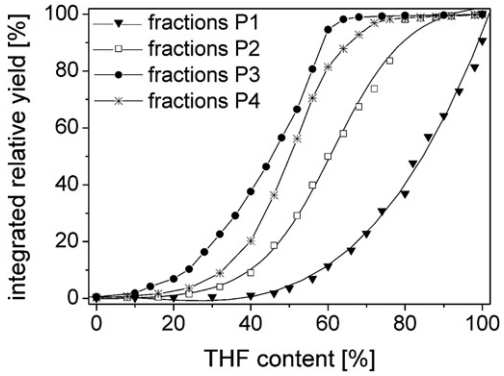

Fig. 4. Elution behavior of the different polymers during fractionation.

Table 3
Comparison of integrated, relative yields during the preparative fractionations and molar masses for **P1**–**P4** at a fixed THF content of 60% (v/v) in the eluent.

Starting sample	Integrated relative yield [%]	M_w [g/mol]
P1	11.3	1600
P2	50.0	9600
P3	94.6	167 900
P4	81.5	8900

Source of this kind of information are dilute solution measurements of molar mass dependent viscosity and molecular size. Furthermore, molecular dynamic (MD) simulations could provide visualization of the shape of the polymers in solution. For extensive understanding of the solution behaviour of **P1**–**P4**, we compared both, MD simulation and experimental data in solution.

3.3.1. MD simulation

The molecular dynamic simulations were carried out for models of **P1**–**P4** in dilute solution of THF. The relaxed NpT time average ensemble from 200 to 500 ps, i.e. with constant particle number (N), constant pressure $p = 101.3$ kPa and constant temperature $T = 298$ K as the thermodynamic standard state, was used for statistical evaluation. In Fig. 5 **P1** and **P3** at identical polymerization degree in a dilute THF solution are compared.

Visually, only small differences could be realized between the dissolved molecules. More meaningful is, however, comparison of the monomer density distribution between the different systems. Fig. 6a shows the monomer density across the simulation box relative to the relaxed box length of 7.78 nm (**P1**), 8.17 nm (**P2**), 8.18 nm (**P3**) and 7.18 nm (**P4**). The area occupied by the polymer of 0.25 up to 0.75 relative to the full box shows that the THF fills up the outer region of the simulation box corresponding to a diluted solution system. Fig. 6a is a clear indication that **P1** and **P4** possess nearly identical density distribution with a maximum significantly higher than the distribution of **P2** and **P3**. These data correspond to reduced rinsing of the THF molecules into the macromolecule of **P1** and **P4** compared to **P2** and **P3**. Taking into account Scheme 2 it could be concluded that the acetal protection of the terminal groups has stronger influence on the solvation of the hyperbranched structure in THF than the acetate group protecting the linear units.

Another evaluation of the simulation data could be performed by calculating the radial distribution function (RDF) of the monomers which describes the probability to find two monomers with a given distance between them. Therefore the average atom distance across the molecule independent on the atom types was determined as a time average. In Fig. 6b the corresponding RDF data are presented, showing clear differences. Starting at about 0.4 nm

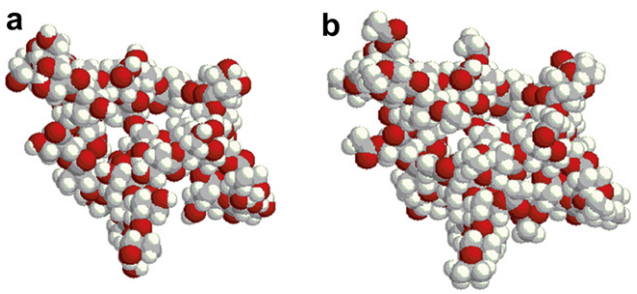

Fig. 5. Calotte model of the relaxed state of **P1** (A) and **P3** (B) after 185 ps simulation time. The solvent molecules of THF are omitted for better visualization of the polymer shape.

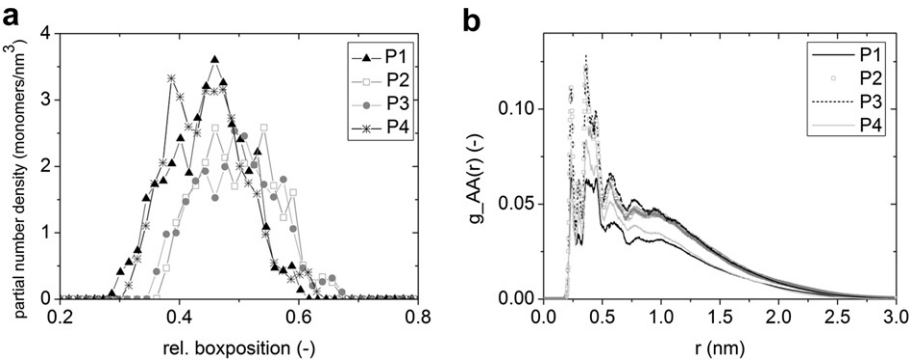

Fig. 6. a) Partial monomer number densities versus the relative position within the simulation box; b) Radial distribution function of the monomers versus the radial distance.

one can distinguish four spheres. Comparing the curves corresponding to **P1** and **P4** increasing state of ordering with the protection of the linear groups can be observed. The effect of ordering is even higher after acetal protection of the terminal groups of **P1** leading to **P2**, but this effect cannot be increased by further protection of the linear groups. The behavior of **P2** and **P3** seems to be nearly the same. The peak positions are similar for all polymers, which shows that no significant changes in the density could be observed at smaller distances. At larger distances the curves resemble the theoretically expected decay of the correlation function [27]. This decay is sensitive to the excluded volume [28,29] and hence it gives the possibility to evaluate this effect. However, at this stage only qualitative estimation could be performed due to lack of data, subject of further extensive study of this behaviour. The curve shape in Fig. 6b leads to the conclusion that **P4** and **P1** possess lower excluded volume than **P2** and **P3**. This effect is supported by the dilute solution experiments described below.

Summarizing the simulation results we can conclude that the chemical modifications have strong influence on the internal ordering state of the hyperbranched polymer. Furthermore, the RDF results are an indication for a liquid like behaviour of the hyperbranched polymer. However, it distinguishes from a real bulky liquid by the decreasing probability with increasing distances. In other words, the hyperbranched polymer behaves similar to a fog like droplet in a gaseous phase.

3.3.2. Molar mass dependence of the intrinsic viscosity

In order to provide experimental validation of the MD simulation results, information about molecular size and intrinsic viscosity should be available. However, because of the relatively small amount of the most of the fractions and the low *dn*/*dc* values of this polymer type, information about the radius of gyration by light scattering cannot be obtained. Nevertheless, the relationship between the intrinsic viscosity and the molar mass, expressed in the Kuhn–Mark–Houwink–Sakurada (KMHS) equation can be used for this purpose:

$$[\eta] = KM^{\alpha} \tag{3}$$

The KMHS exponent α is a parameter corresponding to the compactness and shape of the macromolecules in a certain solvent. In a good solvent, a linear statistical coil would possess α values between 0.5 and 1.0, whereas a sphere-like polymer approaches 0. Typical values for hyperbranched polymers are in the range of 0.3 and 0.5 [30]. These values are commonly obtained by online viscosity measurements using SEC coupled to viscosity, light scattering and RI detectors (triple-SEC), because of the broadly distributed hb polymers and the lack of samples with variable molar masses. Furthermore, the application of triple-SEC saves time-consuming fractionation and investigation of every single fraction. By these online measurements linear KMHS dependencies have been reported for different hb polymers [30,31]. The results from our triple-SEC investigation support these linear relationships as shown on Fig. 7a.

The KMHS exponents were determined for all broadly distributed starting polymers **P1**–**P4** by the online method indicating that depending on the polarity of the end groups the shape of the polymers is clearly changing. In Table 4, the α_{online} values are listed showing that the OH-terminated **P1** possesses evidently more compact shape in THF than the fully protected **P3**. For the α_{online} values fractal dimensions of the polymers could be calculated leading to 2.2 for **P1** and **P4** and approximately 2 for **P2** and **P3**. This fact corresponds to the MD simulation results, showing that with

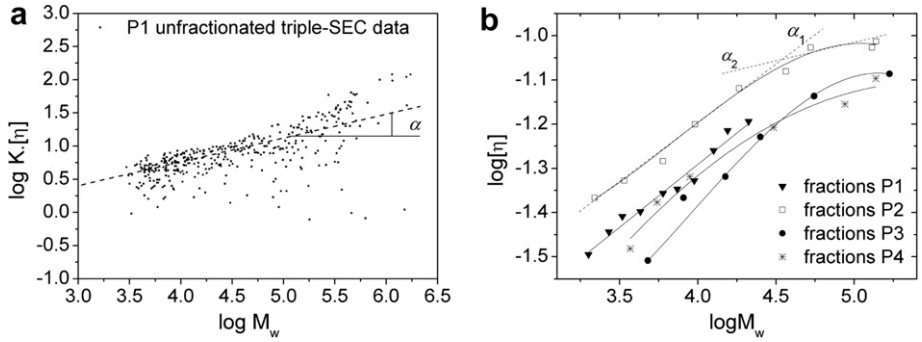

Fig. 7. Kuhn–Mark–Houwink–Sakurada plots of a) the non-fractionated **P1** via SEC-MALLS-viscosity detection (triple-SEC) and linear fit of the data with a slope corresponding to KMHS exponent α; b) the fractionated polymers **P1**–**P4** via offline determination of molar mass and intrinsic viscosity – nonlinear fits should guide the eye; linear fits of both slopes in a non-constant KMHS behavior of **P2** lead to α_1 and α_2 as an example.

Table 4
Kuhn–Mark–Houwink–Sakurada (eq. (3)) exponents for **P1** to **P4** determined online (triple-SEC) or offline (fraction analysis).

Polymer	α_{online} [a]	$\alpha_{1,offline}$ [b]	$\alpha_{2,offline}$ [b]
P1	0.36 ± 0.02	0.28 ± 0.02	–
P2	0.42 ± 0.01	0.27 ± 0.02	
P3	0.53 ± 0.02	0.39 ± 0.04	Approx. 0.1
P4	0.35 ± 0.02	0.36 ± 0.05	

[a] KMHS exponent determined by triple-SEC.
[b] KMHS exponent determined by offline characterization of fractions – α_1 is the first slope, in the low molar mass region, α_2 is the second slope, in the higher molar mass region.

increasing amount of non-polar end groups, the molecules become more expanded and are better flushed by the solvent. This result supports additionally the conclusions from the elution fractionation of **P1**–**P4** that the elution and solubility of larger polymer molecules in THF is increasing at lower end group polarity.

In Fig. 7a one can note strong scattering in the KMHS dependence, which has to be ascribed to the quality of the light scattering signals due to very low contrast (dn/dc) of the polymer in the solvent THF. Furthermore, this leads to limited detection possibility in the beginning and at the end of the distribution, where the concentration of macromolecules is too low for a light scattering response in a good quality. In order to obtain more precise viscosity data in the high molar mass region, offline viscosity characterization of single fractions of **P1**–**P4** has been carried out. For this purpose, not the triple-SEC detection was used, but the viscosity of the fractions was measured in batch. The dependencies of the intrinsic viscosities from the molar masses are presented in a double logarithmic plot in Fig. 7b. For all polymers, a linear KMHS dependence can be observed in the range below approx. 50 000 g/mol. This behavior is changing for **P2**–**P4** at higher molar masses corresponding to change in the molecular shape. We would expect the same characteristics for **P1** as well, whereas this assumption cannot be supported by data due to the lack of higher molar mass fractions of **P1**, as discussed above. A detailed analysis of the KMHS exponents in the lower molar mass range shows similar trend as detected by triple-SEC (Table 4). However, there is a deviation of these values from the online determination for all polymers with exception of **P4**, which could be ascribed to the significantly lower polydispersity leading to reduced co-elution of species with different branching density during the SEC separation process, as explained below.

In contrast to triple-SEC, an additional significant effect visible in Fig. 7b is the strong contraction at higher molar masses leading to α values of about 0.1. The discrepancies in the linearity of the KMHS-behaviour could be explained on the one hand with the limits of the lights scattering signal in higher molar mass region due to low concentrations. On the other hand, the linear KMHS plots from the triple-SEC correspond to previous investigations on hb polymers, as mentioned above. However, the results of the analysis of single fractions from Fig. 7b resemble the theoretical predictions from several simulation studies on the KMHS behavior of dendritic polymers. Independent from the simulation procedure kinetic bead-rod model [32], Brownian dynamics [33,34], or Monte Carlo simulations [35,36] all studies verify a maximum in the intrinsic viscosity with increasing molar mass even at lower DB. Such maximum has been observed experimentally for dendrimers depending on their generation number [37]. However, the experimental reports on hb polymers with narrow distribution and different molar masses are rather rare. Nonlinear KMHS behavior has been reported for hb poly(amidoamines) [38] and for poly(etheramides) [25]. The reasons for the differences between the triple-SEC results and the results from the single fraction analysis should be searched in the influence of the multiple distributions (DB, molar mass etc.) represented in an original hyperbranched sample. During SEC separation, simultaneous elution of molecules with similar hydrodynamic radius but different degree of branching is possible leading to overlap of distributions of different origin. Applying preparative fractionation, separation according to one dimension (molar mass) can be confirmed, which does not exclude the existence of DB distribution in one fraction. However, in our case this distribution is obviously comparable for all fractions, as NMR calculations confirmed (Table 2). Two-dimensional chromatographic separations should elucidate this still questionable behavior, which is the purpose of our future investigations on the basis of the model polymers presented in this work.

The more open shape of the completely modified polyester **P3** is confirmed by the high value of $\alpha = 0.39$ in the lower molar mass region. This value is approaching exponents rather typical for statistical linear coil in theta-conditions. Comparison of the compactness of the hb polymer to its linear analogue could shed light on the influence of the dendritic architecture on the KMHS behavior. For this purpose, linear polyester, synthesized and characterized in a previous work [19] and shown in Fig. 8b has been used. The KMHS relations of both, linear polyester and **P3**, are plotted in Fig. 8a showing linear dependence in the complete molar

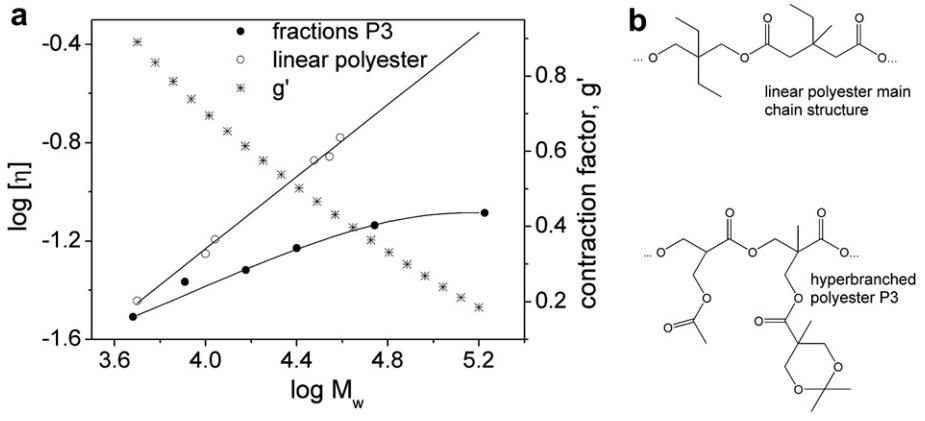

Fig. 8. a) Determination of the contraction factor of **P3** depending on the molar mass on the basis of viscosity data of linear polyester with analog chemical structure. b) Schematic comparison of the main chain structure of the linear and hyperbranched polyester.

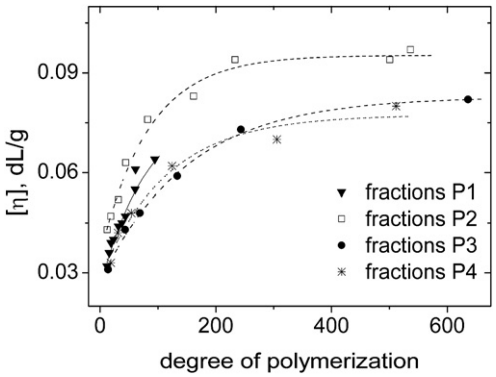

Fig. 9. Intrinsic viscosity dependence from the degree of polymerization (DP) for the fractionated polymers **P1**–**P4**. Intrinsic viscosity was determined offline and DP was calculated from M_n (SEC-MALLS, see Experimental section) and the number of dendritic (22%), terminal (23%) and linear (55%) units as determined by ^{13}C NMR.

mass region for the linear polymer, as theoretically expected, with $\alpha = 0.73$ corresponding to linear coil in a good solvent. One could note that the end group influence of both polymers should be comparable in order to exclude any other effects apart from branching. And indeed, while the hb **P3** is completely non-polar, the linear polyester still possesses two polar end groups per molecule. In reality, we cannot expect that these two end groups could significantly influence the solution behavior of the polymer especially at the represented, high molar masses. Hence, the contraction of the hb polyester can be calculated according to Eq. (4) after fitting the viscosity data of the **P3** fractions and the linear polyesters with different molar mass:

$$g' = \frac{[\eta]_{\text{branched}}}{[\eta]_{\text{linear}}} \tag{4}$$

The contraction factor decreases with the molar mass to approx. $g' = 0.1$, which corresponds to very strong contraction at molar masses higher than 150 000 g/mol, taking into account that if no contraction of a branched polymer compared to its linear analogue is occurring, g' remains 1.0. In order to evaluate the level of contraction, comparison with extensively investigated, well-defined star polymers should be made. As an example, stars with three arms have contraction factor of approximately 0.8 [39] whereas 32 arms lead already to 0.2 contraction factor [40].

Even if they possess similar slopes, the KMHS curves of the differently modified polymers are shifted according to their molar mass, and hence, direct comparison and analysis of the role of the end groups is only possible by estimating the KMHS exponents.

In order to exclude the influence of the different molar mass of the end groups and to visualize the change in the intrinsic viscosity for the differently modified polymers, we plotted $[\eta]$ against the degree of polymerization (Fig. 9). Slightly increased intrinsic viscosity after replacement of the terminal OH groups with acetals in **P2** was observed. However, significantly stronger effect can be found after modification of the linear OH- to acetate-groups. The drop in the intrinsic viscosity can be explained with increased solubility of the non-polar macromolecules, as supported by the fractionation analysis, discussed above. An interesting fact is that the intrinsic viscosity dependence of **P4** is as low as for **P3** even though the terminal units were deprotected. This phenomenon shows clearly the role of the terminal and the linear functional groups for the hb macromolecules in solution: the affinity of the linear functional groups to the solvent is evidently overlapping the influence of the terminal end groups. Because of the fact that the polarity of both groups in **P4** is opposite, an explanation of this effect could be the content of the linear (55%) and the terminal groups (23%) as determined by ^{13}C NMR.

4. Conclusions

Selective protection of the linear and terminal end groups of hyperbranched poly(BisMPA) was successfully carried out leading to four types of polymers with variation of the end group polarity. Fractionation of all samples was performed according solely to molar mass and leading to fractions with narrow molar mass distribution and identical degree of branching. NMR measurements confirmed 45% degree of branching (DB_{Frey}) and complete modification for all polymer types. Analysis of the elution behaviour of the different samples showed that the separation is strongly depending on the functionality type leading to tunable polymer–eluent interactions. Additional MD simulations of the polymers in dilute solution supported the change of the molecular density depending on the end groups type. The simulation results show that internal ordering state is influenced by the different functionality and the hyperbranched polyesters possess liquid like behaviour. Molar mass dependent viscosity measurements confirmed KMHS-behaviour corresponding to increasingly compact molecular shape at higher molar masses. Deviations in the slope in the lower molar mass region support the MD simulation results and show different solution behaviour depending on the functionality. Comparison to a linear polyester with similar chemical structure enabled determination of the viscosity contraction factor showing very strong contraction of the completely non-polar polymer.

References

[1] McKee MG, Unal S, Wilkes GL, Long TE. Prog Polym Sci 2005;30(5):507–39.
[2] Voit B. J Polym Sci Part A Polym Chem 2005;43(13):2679–99.
[3] Hanselmann R, Holter D, Frey H. Macromolecules 1998;31(12):3790–801.
[4] Hawker CJ, Lee R, Frechet JMJ. J Am Chem Soc 1991;113(12):4583–8.
[5] Frey H, Holter D. Acta Polym 1999;50(2–3):67–76.
[6] Gerber J, Radke W. Polymer 2005;46(22):9224–9.
[7] Al Samman M, Radke W, Khalyavina A, Lederer A. Macromolecules 2010;43:3215–20.
[8] Edam R, Meunier DM, Mes EPC, Van Damme FA, Schoenmakers PJ. J Chromatogr A 2008;1201(2):208–14.
[9] Flory PJ. Principles in polymer chemistry. Ithaca, New York: Cornell University Press; 1953.
[10] Malmström E, Hult A. Macromolecules 1996;29(4):1222–8.
[11] Magnusson H, Malmström E, Hult A. Macromolecules 2000;33(8):3099–104.
[12] Burgath A, Sunder A, Frey H. Macromol Chem Phys 2000;201(7):782–91.
[13] Chikh L, Tessier M, Fradet A. Polymer 2007;48(7):1884–92.
[14] Komber H, Ziemer A, Voit B. Macromolecules 2002;35(9):3514–9.
[15] Lee CC, MacKay JA, Frechet JMJ, Szoka FC. Nat Biotechnol 2005;23(12):1517–26.
[16] Antoni P, Malkoch M, Vamvounis G, Nystrom D, Nystrom A, Lindgren M, et al. J Mat Chem 2008;18(22):2545–54.
[17] Vestberg R, Malkoch M, Kade M, Wu P, Fokin VV, Sharpless KB, et al. J Polym Sci Part A Polym.Chem 2007;45(14):2835–46.
[18] Haag R, Stumbe JF, Sunder A, Frey H, Hebel A. Macromolecules 2000;33(22):8158–66.
[19] Schallausky F. Untersuchung der Eigenschaften von unterschiedlich verzweigten Polyesterstrukturen in Lösung (PhD thesis). TU Dresden: ISBN 978-3-89963-541-6; 2007.
[20] van der Spoel D, Lindhal E, Hess B, Groenhof G, Mark AE, Berendsen HJC. J Comp Chem 2005;26:1701–19.
[21] Berendsen HJC, Postma JPM, van Gunsteren WF, DiNola A, Haak JR. J Chem Phys 1984;8:3684–90.
[22] Schmidt MW, Baldridge KK, Boatz JA, Elbert ST, Gordon MS, Jensen JH, et al. J Comp Chem 1993;14:1347–63.
[23] Greene TW, Wuts PGM. Protective groups in organic synthesis. New Jersey: John Wiley & Sons; 1999.
[24] Zagar E, Grdadolnik J. J Mol Struct 2003;658(3):143–52.
[25] Lederer A, Voigt D, Clausnitzer C, Voit B. J Chromatogr A 2002;976(1–2):171–9.
[26] Lederer A, Elrehim MA, Schallausky F, Voigt D, Voit B. e-Polymers; 2006.
[27] de Gennes PG. Scaling concepts in polymer physics. Ithaca and London: Cornell University Press; 1979.
[28] Freltoft T, Kjems JK, Sinha SK. Phys Rev B 1986;33(1):269–75.

[29] Burchard W. Macromolecules 2004;37(10):3841–9.
[30] Mori H, Müller AHE, Simon PFW. In: Leibler L, editor. Macromolecular engineering: precise synthesis, materials, properties, applications. Weinheim: Wiley-VCH; 2007. p. 973ff.
[31] Turner SR, Voit BI, Mourey TH. Macromolecules 1993;26(17):4617–23.
[32] Aerts J. J Comp Theor Polym Sci 1998;8(1–2):49–54.
[33] Lyulin AV, Adolf DB, Davies GR. Macromolecules 2001;34(11):3783–9.
[34] Sheridan PF, Adolf DB, Lyulin AV, Neelov I, Davies GR. J Chem Phys 2002;117(16):7802–12.
[35] Widmann AH, Davies GR. Comput Theor Polym Sci 1998;8(1–2):191–9.
[36] Mourey TH, Turner SR, Rubinstein M, Frechet JMJ, Hawker CJ, Wooley KL. Macromolecules 1992;25(9):2401–6.
[37] Tomalia DA, Hedstrand DM, Wilson LR. Encyclopedia of polymer science. New York: Wiley; 1990.
[38] Hobson LJ, Feast WJ. Chem Commun 1997;21:2067–8.
[39] Berry GC. J Polym Sci Part A-2: Polym Phys 1971;9(4):687 [&].
[40] Zhou LL, Hadjichristidis N, Toporowski PM, Roovers J. Rubber Chem Tech 1992;65(2):303–14.